

Efficient R-peak Detection Algorithm for Real-time Analysis of ECG in Portable Devices

C. Crema, A. Depari, A. Flammini, A. Vezzoli

Department of Information Engineering
University of Brescia
Brescia, Italy
alessandro.depari@ing.unibs.it

Abstract—Detection of R-peaks in an electrocardiogram (ECG) acquisition is the primary goal of any algorithm for the automatic processing of ECG signals. Several methods have been proposed in the past to accomplish this task, but usually they are designed for the use in clinical situations, where strict real-time requirements are not always needed and availability of devices with high computational resources is not a problem. The recent and broad success of personal and portable devices for health monitoring has opened a new scenario, in which new algorithms need to be developed in order to satisfy constraints due to limited computational resources and the need of having embedded and real-time data processing. This work describes an efficient algorithm for the R-peak detection, designed for low-cost and low-performing portable devices. Performance of the proposed approach, evaluated with a set of well-known ECG waveform, is comparable with traditional methods found in literature. Finally, the successful implementation of the algorithm in a smartphone-based low-cost ECG acquisition system has validated the feasibility of the proposed approach.

Keywords— *R-peak detection; embedded ECG analysis; wearable systems.*

I. INTRODUCTION

The electrocardiographic signal (ECG), being a representation of the heart activity, is one of the most important bio-signals used for the analysis and monitoring of health conditions of living beings [1]. It derives from capturing small electrical signals generated by movements of heart muscles and propagating through the body until the skin. Alteration of the normal heart functionalities reflects on the generated electrical signals, and thus on the acquired ECG; the analysis of ECG waveform is a primary instrument for monitoring of the heart activity and discovering heart pathologies.

ECG is usually acquired by a 10-electrode system, which originates 12 differential electrical signals, currently referred as ECG leads. The placement of electrodes on the body and the way of electrode coupling follow a standard scheme, which guarantees a view through different planes and thus a comprehensive observation of the heart activity. However, such an accurate and complete acquisition is necessary only for specific situations; a subset of electrodes (typically 3, 4 or 5) can be used to acquire a limited number of leads thus

reducing the complexity of the acquisition system [2].

In an ECG acquisition, the QRS complex and, in particular, the position of its peak (R-peak) is the most evident feature. The distance between consecutive R-peaks (RR period) is a very important parameter in the analysis of heart pathologies [1]. RR period can be used for monitoring heart rate variability (HRV), one of the most valuable markers for detecting arrhythmias, for noticing abnormal heart rhythm (bradycardia/tachycardia), and for locating premature ventricular contractions and night pauses [3]. The parametric study of the ECG morphology is usually performed starting from the detection of the time positions of R-peaks.

Traditionally, ECG acquisition and processing is performed in medical environment, where specialized personnel can carefully analyze traces from a 12-lead ECG. This work is particularly burdensome and prone to errors, especially if long-term acquisitions need to be analyzed. For this reason, in the last decades, support tools have been introduced to assist cardiologists with an automatic ECG feature detection. As an example, Holter portable systems for the prolonged monitoring of heart activity are usually sold together with their own signal processing software, which automatically extracts the most significant parameters as well as provides different tools to facilitate the manual ECG analysis [4]. Being such tools oriented to the use in medical and clinical environment, processing algorithms are developed privileging performance more than computational resource optimization. Real-time processing aspect is also not a priority in this kind of applications.

In the recent years, thanks to the decrease of price of processing unit devices and the quick and broad success of personal smart devices (smartphones, tablets, smartwatches...) there has been an increasing interest for the concept of telemedicine and mobile health (m-health). In such a context, the possibility of having a basic, but real-time, local processing of the acquired bio-signal data, for informative and pre-alert purposes, becomes of primary importance [5], [6]. Constraints due to the relatively limited computational capacity of such devices have to be taken into account for the development of suitable processing algorithm. Further complications arise from the fact that usually bio-signals are acquired using non-professional and low-cost sensor systems and that the subject under observation is potentially

This work has been partially supported by Smart Cities and Communities and Social Innovation Grant D84G14000220008: "Smart Aging", and by the EULO Grant D88C13000050005: "Smart ECG: uno strumento miniaturizzato ad elevate efficienza energetica per il monitoraggio a lunghissimo termine dell'elettrocardiogramma: aspetti tecnologici, clinici e scientifici".

performing some kind of movements; those facts can determine a very noisy and low-quality acquired signal.

In this work, an algorithm for real-time R-peak detection suitable for embedded devices used in portable equipments is proposed. In particular, the system described in [7] has been considered as a test case. For the design of the algorithm, the aforementioned aspects related to the real-time processing, noisy signals and relatively low computational resources have been taken into account. The algorithm has been also validated with ECG acquisition from the MIT-BIH arrhythmia database [8], [9] and compared with performance of different approaches found in literature.

The paper is structured as follows: in Section II, the most significant and widespread R-peak detection algorithms found in literature are described; the detailed explanation of the proposed method can be found in Section III; the experimental setup for the algorithm validation and comparison with methods in literature is presented in Section IV, whereas experimental results and comments are located in Section V. Finally, some conclusions are drawn.

II. R-PEAK DETECTION METHODS

Several algorithms for the automatic detection of R-peaks have been proposed during the last three decades. The most significant and widely used ones are described in this section.

A. Pan-Tompkins

This algorithm was developed in 1985. The ECG track is first filtered, differentiated and then squared; this signal is then integrated by a moving-window integrator. Two sets of thresholds are used to detect the QRS complexes: one works with the filtered ECG, and the other one with the signal produced by the moving window integrator. The dual-threshold technique is used to find missed beats, thus reducing false negatives. The thresholds continuously adapt to the characteristics of the signal, since they are based on the most recent signal and noise that are detected in the process. RR period is constantly compared with averaged RR, so if a QRS happens too late, a lower threshold is applied to that portion of signal, to be sure if the missed QRS is a false positive or not [10].

B. Wavelet-based Algorithms

Many methods use Wavelet transform to detect R-peaks; Li et al. [11] wrote the first important work about this topic. The wavelet transform is defined as the integral of the product between a signal and a function called mother wavelet; discrete wavelet transform results from discretized scale and translation parameters, and most of the times is implemented using a dyadic filter bank. This operation decomposes the ECG signal into elementary blocks, well located both in time and in frequency; the analysis of these blocks allows to distinguish ECG waves from noise, artifacts and baseline drift, making R-peak detection easier. One example of wavelet-based algorithm is reported in [12]. In this work, after the ECG is wavelet-transformed and divided into sections, with one R-peak each ideally, a threshold, calculated with an autoregressive algorithm, is applied to it to find the R-peak. If no

peak is found in the section, the search is re-done up to three times with a lower threshold.

C. Empirical Mode Decomposition

Another method to analyze an ECG is to use empirical mode decomposition (EMD), which is a data-driven process to expand data in terms of intrinsic mode functions (IMFs), as reported in [13]. In this work, the goal is to use EMD to create an algorithm robust to electromyogram-like noise, generated by electrical activity of skeletal muscles. The envelopes of the local maxima and minima of the signal $X(t)$ can be used to calculate the first IMF with a process called sifting [14]. The first IMF contains oscillations at high frequencies, and it can be subtracted to the original signal to obtain a residue, r_1 . The sifting can be applied on r_1 , obtaining all the IMFs of the signal. In the end, they can be processed and analyzed to find the R peaks, usually with a threshold method, as reported in [15].

D. Area Over the Curve

This method, reported in [16], derives from the need of finding an algorithm not requiring burdensome pre-processing or complex mathematics for detecting R-peaks, because it is supposed to be used in portable devices for telemedicine. The basic concept of this method comes from the fact that QRS complexes can be identified very easily by humans, due to their characteristic shape, narrow and tall. Authors create the notion of *area over the curve*, which basically is the empty area around a local maximum; this area is larger in tall and narrow peaks (such as QRS complexes) than it is in wider or small ones (respectively, T and P waves). This area is calculated for every local maximum, and then sorted in a decreasing way. Every area that is above a certain threshold corresponds to an R-peak, and the rest are other component of the ECG (e.g., P or T waves) or isolated spiky noise. The statistical parameters obtained with this algorithm are not as good as the most promising detection techniques reported in literature; however, this method represents a good trade-off between performance and computational complexity.

III. THE PROPOSED ALGORITHM

As already mentioned, for the implementation of the proposed algorithm, aspects related to the real-time processing, noisy signals, and relatively low computational resources have been taken into account. The need for real-time processing leads to run the algorithm on signal windows, with duration on the order of tens of seconds. The designed solution is oriented to keep low the computational load, and thus to make suitable the implementation in embedded systems and smart devices, such as smartphone and tablets.

The proposed algorithm is performed in two steps; the first step is devoted to signal filtering and to calculate a set of parameters, which will be used in the second step to actually detect the R-peaks. A comprehensive description of the proposed algorithm, the block scheme of which is shown in Fig. 1, will be given in the following.

A. Pre-elaboration

The first step of signal processing is the elimination of the baseline variability. In particular, the first stage (*HPF* in Fig. 1) filters the input *ECG Signal* exploiting a high-pass FIR filter, designed to keep the computational complexity as low as possible; the width of the moving window of the filter is composed of only two unitary points, reducing the number of sums and avoiding the multiplications. This filter represents an approximation of the differential calculus and its aim is to highlight the slope steepness of the original signal. For the subsequent parts of the algorithm description, the output of this stage will be called differentiated signal (*d_sign*).

The second stage (*Sum* in Fig. 1) returns the indicator *n_ind* related to the noise level of the input signal. In order to reduce the number of operations and avoid multiplications, a row estimation of the noise at high frequencies, obtained by summing the absolute values of *d_sign*, is provided.

In the stage *Comp*, the noise level indicator *n_ind* is compared with a set of thresholds tuned according to the characteristics of the acquisition system. This step produces two filter parameters (F_C and W_W) and two weight coefficients (W_MAX , W_MIN) used in the subsequent stages.

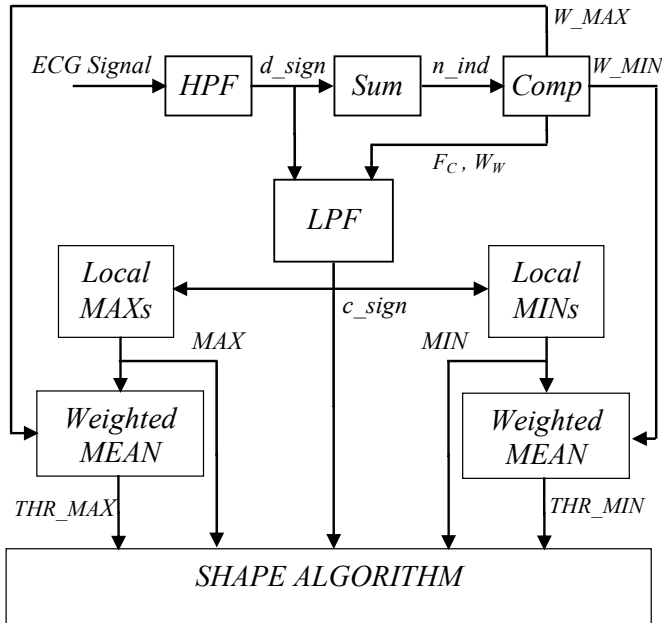


Fig. 1. Schematic of the R-peak detection algorithm.

A low-pass FIR filter (*LPF*) is then used to process the differentiated signal *d_sign* to obtain the so-called conditioned signal *c_sign*; the cut-off frequency F_C and the width W_W of the moving windows are reckoned in the *Comp* stage. The filter tuning is effective because the signal under elaboration is few tens of seconds long, thus the algorithm is able to dynamically deal with the time-variant noise.

The conditioned signal *c_sign* is then processed by *Local MAXs* and *Local MINs* blocks, to obtain two vectors, *MAX* and *MIN*, containing the local maximums and minimums, respectively. The means of the *MAX* and *MIN* are then weighted by the two *Weighted MEAN* blocks using the

coefficients W_MAX and W_MIN calculated in *Comp*. In this way the two scalar values THR_MAX and THR_MIN are obtained.

The conditioned signal *c_sign*, its local maximum and minimum vectors *MAX* and *MIN* as well as the weighted means THR_MAX and THR_MIN are the parameters provided to the stage devoted to the actual detection of the R-peaks.

B. Shape Algorithm

This stage performs the R-peak detection starting from the information provided by the previous processing steps; the output of this block is the indication of the time occurrences $t(BEAT)$ of the input samples which are detected as the peaks of the QRS complexes. Since the shape of the QRS complex can vary according to the electrode position and the pathology of the subject under observation, the proposed algorithm has been designed to properly work with a set of three typical shapes, shown in the insets of Fig. 3, Fig. 4, and Fig. 5. The pseudo-code describing the operations performed by the *Shape Algorithm* block is shown in Fig. 2. The parameter THR_MAX_NB is obtained by halving THR_MAX .

```

for each MIN < THR_MIN
  if
    exist (MAXp: (t(MINi) - ΔMX_PMX < t(MAXp) < t(MINi) - ΔMN_PMX)
    && MAXp > THR_MAX)
    && exist MAXf: (t(MINi) + ΔMN_FMX < t(MAXf) < t(MINi) + ΔMX_FMX)
  then
    t(BEAT) = t(MAXp) < t < t(MINi): c_sign(t-δ) > 0 && c_sign(t+δ) < 0
  else if
    exist (MAXp: (t(MINi) - ΔMX_PMX < t(MAXp) < t(MINi) - ΔMN_PMX)
    && MAXp > THR_MAX_NB)
    && exist MAXf: (t(MINi) + ΔMN_FMX < t(MAXf) < t(MINi) + ΔMX_FMX)
    && MAXf > THR_MAX_NB
  then
    t(BEAT) = t(MINi) < t < t(MAXf): c_sign(t-δ) < 0 && c_sign(t+δ) > 0
  else if
    exist MAXf: (t(MINi) + ΔMN_FMX < t(MAXf) < t(MINi) + ΔMX_FMX)
    && MAXf > THR_MAX
  then
    t(BEAT) = t(MINi) < t < t(MAXf): c_sign(t-δ) < 0 && c_sign(t+δ) > 0

```

Fig. 2. Pseudo-code of the shape algorithm.

The *for* loop scans all the local minimums *MIN* and look for a triplet composed of a local minimum MIN_i and two surrounding local maximums MAX_p and MAX_f (MAX_p preceding MIN_i and MAX_f following MIN_i) which fit the requirements for the detection of a particular QRS shape.

These requirements include temporal position and amplitude difference among the three MIN/MAX points. In particular, such samples have to occur in the temporal windows defined by the following constants: Δ_{MX_PMX} (maximum distance between MIN_i and MAX_p), Δ_{MN_PMX} (minimum distance between MIN_i and MAX_p), Δ_{MX_FMX} (maximum distance between MIN_i and MAX_f) and Δ_{MN_FMX} (minimum distance between MIN_i and MAX_f).

Amplitude difference between samples is evaluated with respect to the previously defined threshold THR_MAX or THR_MAX_NB , according to the QRS shape under investigation. Once a valid triplet is found, the R-peak is

detected by searching for the c_sign zero-crossing among the two maximums; if two zero-crossings are found, the selection is made according to the QRS shape under investigation.

Examples of the application of the algorithm are reported in Fig. 3, Fig. 4, and Fig. 5, where the three different situations of QRS shape shown in their respective insets are considered. The three figures clearly display the detection of the shape fitting with the first, the second and the third if/else requirement described by the pseudo-code of Fig. 2.

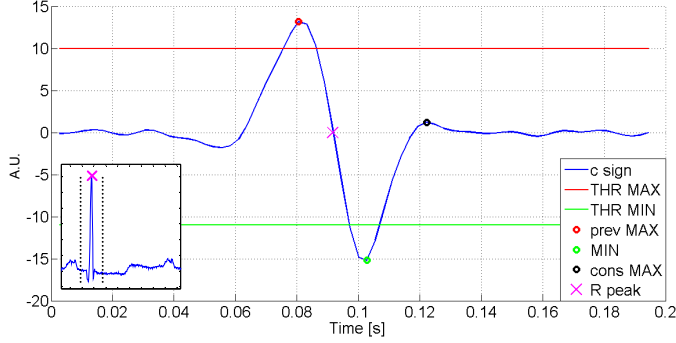


Fig. 3. R-peak detection in a QRS complex with first type shape (in inset).

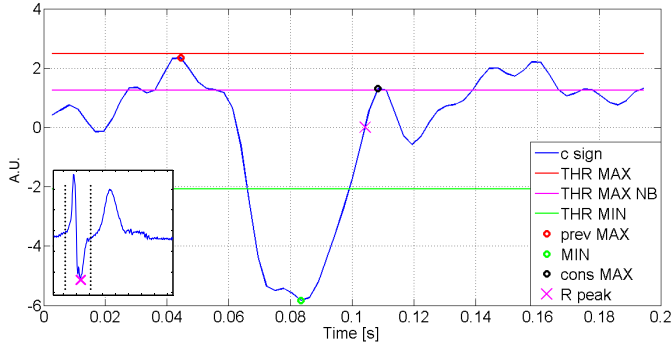


Fig. 4. R-peak detection in a QRS complex with second type shape (in inset).

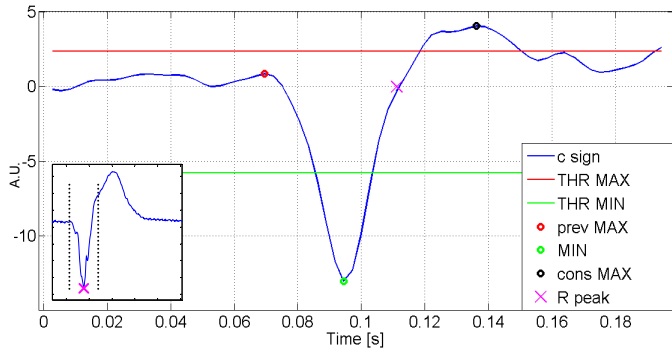


Fig. 5. R-peak detection in a QRS complex with third type shape (in inset).

IV. VALIDATION

To evaluate the performance of the R-peak detection algorithm, it is important to identify the number of correctly detected peaks (true positives, TP), the number of missed peaks (false negatives, FN) and the number of falsely detected peaks (false positives, FP). Starting from these values, it is

possible to reckon the precision and recall indicators, defined by equations (1) and (2), respectively:

$$P = \frac{TP}{TP + FP} \quad (1)$$

$$R = \frac{TP}{TP + FN} \quad (2)$$

Precision gives an indication of how many detected peaks are relevant (high precision means that a high percentage of detected beats are true positives), whereas recall expresses how many relevant peaks are detected (high recall means that a high percentage of beats are detected). The proposed algorithm has been validated using a broad range of ECG signals acquired with a portable acquisition system based on a smartphone. Moreover, to demonstrate the general applicability of the designed method and to compare performance with the algorithms mentioned in Section II, additional tests have been carried out using ECG acquisitions from the MIT-BIH database.

A. Analysis on Portable System Acquisitions

The portable ECG acquisition system considered in this paper is composed of an elastic belt with four embedded electrodes, which are in contact with subjects' chest [7]. Electrodes are located in order to obtain signals in a limb lead fashion. Two electrodes identified as RA (right arm) and LA (left arm) pick up the ECG signal, which is amplified and filtered by an analog conditioning circuit; the electrode RL (right leg) is used as feedback voltage reference on the body of the subject (with a driven right leg circuit), whereas the fourth electrode, LL (left leg) is currently not used. The single-lead ECG signal (lead I) obtained with this configuration is then acquired via an audio cable by a smartphone, which automatically processes it to detect heart abnormal activity. Most of serious heart pathologies cannot be identified by using a single-lead ECG; however, this equipment has been designed for the use on subjects recovering from heart accidents, when they are not exposed to an immediate health risk, but anyway need to be constantly monitored. The use of the system would be of great economic benefit for the healthcare system, since subjects can be monitored at home, without the need of hospitalization.

A broad set of acquisitions with different situations have been performed with the system in [7], ranging from hospitalized subjects to non-professional racecar drivers [17]. Traces have been manually analyzed to identify beats and thus to define a reference for the performance evaluation of the proposed algorithm. Signal quality, and hence the obtained algorithm performance, significantly vary among the considered acquisitions. The main source of noise is the movement of the subject, which causes a non-perfect electrodes' adherence and thus artifacts in the acquired signal. For sake of shortness, only three examples, related to different noise levels (clean signal, noisy signal, very noisy signal), are reported in Section V.

B. Analysis on MIT-BIH Database

To demonstrate the general applicability of the proposed method, the MIT-BIH arrhythmia database [9] has been used. This database, created in the late 70's by the Arrhythmia Laboratory of Boston's Beth Israel Hospital (BIH), contains 48 ECG tracks; each of them is recorded at 360 Samples/s and it is 30 minutes long, for a total of about 110000 beats. Among all these acquisitions, 23 tracks were randomly chosen from a collection of over 4000 Holter tapes, and the other 25 ones were selected to include examples of uncommon but clinically important arrhythmias that would not be well represented in a small random sample. The subjects included 25 men aged 32 to 89 and 22 women aged 23 to 89. After the tracks were recorded, two cardiologists worked on them independently, classifying every beat and adding annotations to the tracks. This dataset was used for comparison with state-of-the-art algorithms as described in literature.

C. Smartphone Implementation

The proposed algorithm, designed and tested in MATLAB environment, has been implemented and verified in the smartphone managing the test case system [7], [17]. The smartphone is the LG Optimus L4 II (E440), equipped with a single-core 32-bit 1 GHz ARMv7 processor and 512 MB RAM memory. The Operating System is Android OS version 4.1.2. MATLAB scripts have been developed taking care of developing a code structured Android-compatible. At first, tests in Android environment have been performed offline using a subset of the ECG records employed for the algorithm validation in MATLAB and comparing the obtained results. Furthermore, run-time performance has been evaluated by measuring the algorithm execution time in a real case scenario. ECG signal was therefore acquired with the system in [7] and processed in real-time with a moving window of 4800 Samples, which corresponds to about 12 s (as mentioned in [17], ECG sample frequency is not uniform and it is around 400 Sample/s).

V. RESULTS AND DISCUSSION

Results and comments on tests described in Section IV are presented in the following.

A. Portable System Acquisition Tests

When the noise level is low, as in the case of Fig. 6, the algorithm can correctly detect all the R-peaks. Performance indicators P and R evaluated on acquisitions of this kind lead to values very close to 100%.

Thanks to the adopted signal filtering and the shape detection algorithm, peak detection works properly also when the signal is affected by artifacts and noise. As an example, Fig. 7 shows the R-peak detection for a waveform with moderated artifact level; in this case, all R-peaks are correctly identified. In general, for the acquisitions with such kind of noise level, P and R values of about 98% have been obtained.

However, in particular circumstances, when the signal is quite affected by artifacts and the noise frequency is in the same bandwidth of the QRS complex, the algorithm can

incorrectly identify wrong R-peaks (false positives) or miss correct ones (false negatives). An example of very noisy waveform with both false positives and negatives is shown in Fig. 8. In the acquisitions with such high level of noise and artifacts, P and R indicators values dropped down to 90%.

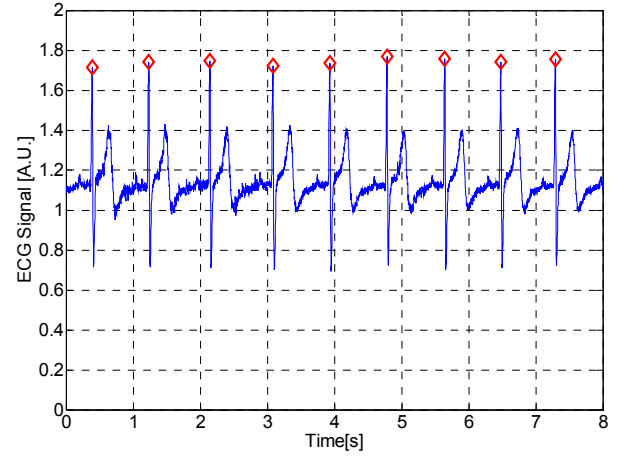


Fig. 6. ECG acquisition with very low noise level; detected R-peaks are annotated with red squares.

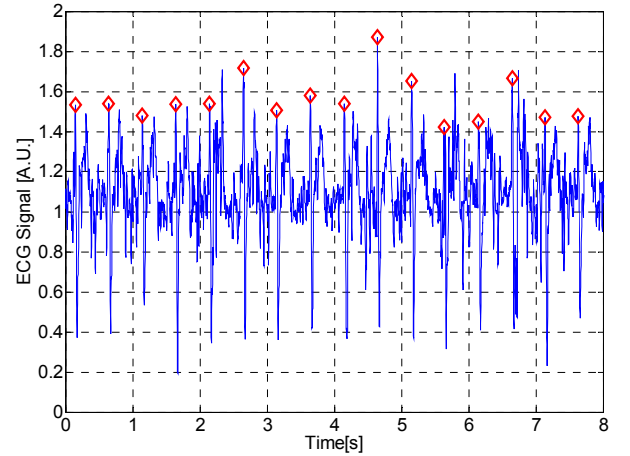


Fig. 7. Noisy ECG acquisition; the positions of detected R-peaks are annotated with red squares.

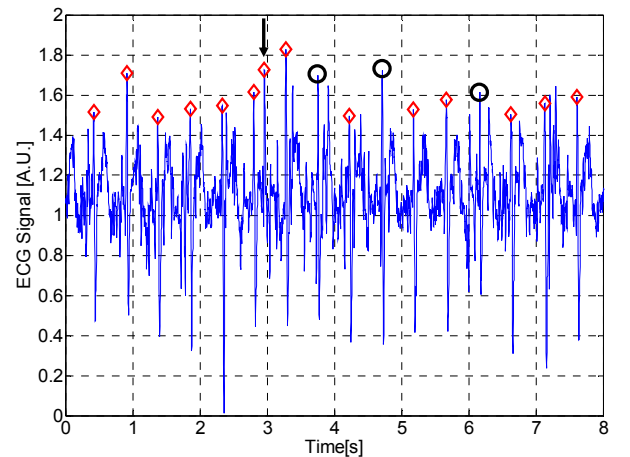


Fig. 8. Very noisy ECG acquisition; the positions of detected R-peaks are annotated with red squares, false positive is pointed with an arrow, and false negatives are annotated with black circles.

It should be noticed that portable systems for health monitoring are usually employed in non-critical situations; such low performance level with very noisy signals can be therefore tolerated. To partially mitigate the problem, without enhancing the algorithm complexity or increasing the system cost, it would be possible to define a confidence indicator related to the noise level (e.g., parameter n_ind in Fig. 1) or to additional acquired information (e.g., the energy of accelerometers placed on the subject). In that way, results related to an acquisition or a portion of it could be marked as unreliable, thus avoiding wrong results to be taken into account.

B. MIT-BIH Database Tests

TABLE I shows the comparison between the results obtained by the proposed algorithm and the performance of the methods presented in Section II, as reported in literature. All the indicators here presented are obtained using the whole dataset of the MIT-BIH arrhythmia database, except for results of [15], where an arbitrary subset of 21 out of 48 records has been considered. Thus, for comparison purposes, results related to [15] in TABLE I has to be considered as a best performance indicator.

TABLE I COMPARISON OF THE PROPOSED R-PEAK DETECTION ALGORITHM WITH METHODS FROM LITERATURE ON THE MIT-BIH DATABASE

Method	Prec. (%)	Recall (%)
Pan-Tompkins [10]	99.56	99.76
Wavelet [12]	99.88	99.90
Empirical mode decomposition [15]	99.96	99.88
Area over the curve [16]	99.3	98.6
Proposed method	99.23	99.05

The proposed method shows slightly inferior performance with respect to the other algorithms. However, it should be underlined that, conversely to the cited methods, the proposed algorithm has been designed to be run in real-time by devices with limited computational capacity; for this reason, the obtained performance can be considered satisfactory, thus validating the effectiveness of the proposed approach.

C. Smartphone Implementation Tests

Comparison between the results of the algorithm performed in MATLAB and Android have shown a perfect adherence, thus demonstrating the correctness of the porting in Android. Run-time of the algorithm routine has been estimated by using the functionality of “Debug” Android class, which allows to timestamp the execution of system threads. On signal windows of about 12 s, the run-time of the algorithm has been evaluated of about 800 ms. It should be noticed that this estimation has been performed when the Android App managing the whole system is fully operative, thus it includes some overhead due to signal acquisition, storage and data communication, executed on concurrent threads. Furthermore, the “Debug” tool also affects the App execution time. Being the real-time factor less than $0.67\times$, the effectiveness of the proposed algorithm for real-time data processing in Android devices has been demonstrated.

VI. CONCLUSIONS

In this paper, an R-peak detection algorithm suitable to be implemented in portable ECG acquisition systems is presented. The algorithm has been designed in order to be run in real-time also by low-performing and thus low-cost devices. As a test case, a low-cost portable ECG acquisition system based on an entry-level smartphone has been considered. Algorithm performance is very good with moderated noisy signal, whereas it considerably suffers when dealing with acquisitions affected by high levels of artifacts. The proposed approach has been also compared with other algorithm found in literature (not specifically designed for portable systems), by using a standard set of ECG acquisitions. Despite the lower computational complexity, performance of the proposed algorithm is comparable with the considered algorithms, thus confirming the general validity of the presented approach.

REFERENCES

- [1] Braunwald E. (ed), “Heart Disease: A Textbook of Cardiovascular Medicine”, Fifth Edition, Philadelphia, W.B. Saunders Co, 1997.
- [2] P. D. Purves et al., “Cardiac Electrophysiology – A Visual Guide for Nurses, Techs, and Fellows”, Cardiotext Publishing, 2011.
- [3] Task Force of the European Society of Cardiology and the North American Society of Pacing and Electrophysiology, “Heart rate variability: Standards of measurement, physiological interpretation and clinical use”, *Circulation* 1996, vol. 93, pp. 1043–1065.
- [4] http://www.cardiolineus.com/brochures/brochure_3844_a.pdf
- [5] <https://www.fitbit.com/it/surge#specs>
- [6] <http://www.st.com/web/en/press/t3419>
- [7] A. Depari, A. Flammini, E. Sisinni, and A. Vezzoli, “A wearable smartphone-based system for electrocardiogram acquisition,” *IEEE International Symposium on Medical Measurements and Applications Proceedings (MeMeA)*, Lisbon, Portugal, June 11-12, 2014, pp. 54-59.
- [8] Goldberger A. L. et al., “PhysioBank, PhysioToolkit, and PhysioNet: components of a new research resource for complex physiologic signals,” *Circulation*, vol 101, e215-e220, 2000.
- [9] G. B. Moody and R. G. Mark, “The impact of the MIT-BIH Arrhythmia Database,” *IEEE Engineering in Medicine and Biology*, vol. 20, no. 3, pp. 45-50, May/June 2001.
- [10] J. Pan and W. J. Tompkins, “A Real-Time QRS Detection Algorithm,” *IEEE Trans. Biomed. Eng.*, vol 32, pp 230-236, March 1985.
- [11] C. Li, C. Zheng, and C. Tai, “Detection of ECG characteristic points using wavelet transforms,” *IEEE Eng. Med. Biol. Mag.*, vol 42, pp. 21-28, January 1995.
- [12] M. Rooijakkers, C. Rabotti, M. Bennebroek, J van meerbergen, and M. Misch, “Low-complexity R-peak detection in ECG signals: A preliminary step towards ambulatory fetal monitoring,” *Engineering in Medicine and Biology Society, EMBC, 2011 Annual International Conference of the IEEE*, pp. 1761-1764, August 2011.
- [13] A. J. Nimunkar and W. Tompkins, “R-peak Detection and Signal Averaging for Simulated Stress ECG using EMD,” *Proceedings of the 29th Annual International Conference of the IEEE EMBS*, pp. 1261-1264, August 2007.
- [14] N. E. Huang, et al., “The empirical mode decomposition method and the Hilbert spectrum for non-stationary time series analysis,” *Proc. R. Soc. London A*, vol 454, pp. 903-995, 1998.
- [15] S. Pal and M. Mitra, “Empirical mode decomposition based ECG enhancement and QRS detection,” *Computers in Biology and Medicine*, vol. 42, pp 83-92, 2012.
- [16] Y. Liao, R. Na, and D. Rayside, “Accurate ECG R-Peak Detection for Telemedicine,” *IEEE Canada International Humanitarian Technology Conference (IHTC)*, pp. 1-5, June 2014.
- [17] C. Crema, et al., “Smartphone-based system for the monitoring of vital parameters and stress conditions of amateur racecar drivers,” *IEEE Sensors, Busan, South Korea*, November 1-4, 2015, pp. 1343-1346.